Sheath Overvoltages Due to Faults on An EHV Cable

A. Ametani
Doshisha University
Kyoto 610-03, Japan

C. T. Wan
Hong Kong Electric Co. Ltd.
44 Kennedy Rd., Hong Kong

Abstract

The present paper investigates sheath overvoltages due to faults on a *275kV* underground cable system. A core-to-sheath short-circuit fault generates a higher overvoltage than that due to a core and sheath to ground fault. The highest overvoltage appeared at the next node to the faulty position in a crossbonded cable is the same as that in a normal-bonded cable, and is greater than the sheath insulation level "*60kV*" of a *275kV* cable in Japan. Sheath protection arresters (CCPU) decrease the overvoltage less than the insulation level except the highest overvoltage. Maximum energy absorbed by the CCPU reaches more than *10kJ* which exceeds the limit of an arrester with the operating voltage of *60kV*.

1. Introduction

An increase of extra-high voltage (EHV) underground cable transmission makes it important to investigate transient overvoltages on the cable. A number of works on switching surge overvoltages in cable systems have been carried out, but only few publications on fault surge overvoltages have been found /1-5/.

This paper investigates sheath overvoltages due to a core and sheath to ground fault and a core-to-sheath metallic short-circuit fault, which could occur very rarely under construction of water and gas pipes, building and/or road on a *275kV* underground cable system. The cable system is assumed to be normal-bonded, crossbonded and/or partially crossbonded. The sheath overvoltage distribution along the cable is obtained for various fault positions and phases, and the effect of a sheath grounding resistance and a grounding wire inductance on the sheath overvoltages are studied. Also, the effect of a sheath protection arrester (CCPU) is investigated as a countermeasure to control the sheath overvoltages. Furthermore, a validity of a neutral wire as an alternative to damp the overvoltages is examined.

The fault surge overvoltages are calculated using the EMTP-ATP/6/.

2. Model System

Fig. 1(a) illustrates a model of a *275kV* underground cable system investigated in the paper. L_r and R_r in the figure are a load impedance to represent a load flow before initiation of a fault, and the value are determined based on measured waveforms of fault voltages and current given in Fig. 2. Inductance L_s represents a short-circuit capacity of a source circuit. Each cable sheath is grounded at the both ends through resistance R_g and the grounding wire is modeled by inductance L_g with $1\ \mu H/m$.

Ground and metallic short-circuit faults are assumed to occur at the positive peak of the source voltage following the measured waveforms in Fig. 2.

Fig. 1(b) and (c) shows the cable arrangement and the cross-section respectively, and the corresponding parameters are given in Table 1(a). The characteristic impedance and the modal propagation constants are given in Table 1(b) which are evaluated at frequency $f=1kHz$ considering the power frequency *60Hz* and the dominant transient frequency f_t given by :

$$f_t = 1/4\tau = 6.13kHz$$

where $\tau = (x_1 + x_2 + x_3)/c = 40.8\mu s$,

$$c \cong c_0/\sqrt{\varepsilon_1} = 163m/\mu s$$

c_0 : light velocity in free space,

x_i : cable length in Fig. 1(a)

The parameters are calculated using the CABLE PARAMETERS and the FTP-CABLE CONSTANTS /7,8/.

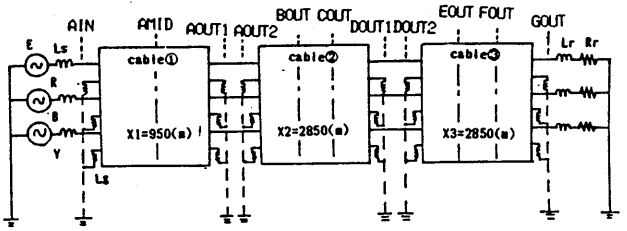

(a) A model circuit (E=224.5kV)

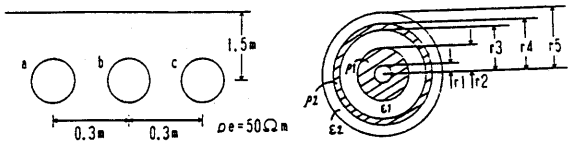

(b) Cable arrangement (c) Cable cross-section

Fig. 1 A 275kV CV cable

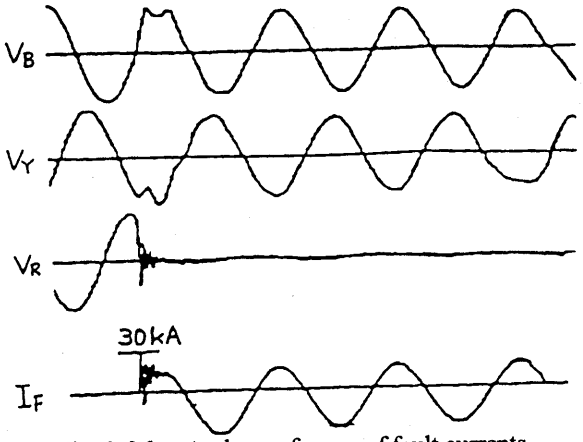

Fig. 2 Measured waveformes of fault currents and voltages

Table 1 Cable parameters

(a) Configuration

r1 = 7.0mm	ε1 = 3.4
r2 = 23.4mm	ε2 = 7.0
r3 = 40.9mm	ρ1 = 1.724×10-8 Ω-m
r4 = 45.5mm	ρ2 = 2.83×10-8 Ω-m
r5 = 56.05mm	ρe = 50 Ω-m

(b) Parameters at f = 1kHz

(i) Actual characteristic impedance [Ω]

(Zaa)cc = 45.26 = (Zbb)cc

(Zcc)cc = 44.45

(Zaa)aa = 25.77 = (Zbb)aa

(Zcc)aa = 24.94

(Zab)cc = 11.18, (Zac)cc = 9.03

(Zab)aa = 11.12, (Zac)aa = 9.06

(ii) Modal parameters

mode	1	2	3	4	5	6
charact. imp.	16.23	8.36	8.71	6.79	9.67	12.56
velocity (m/ μs)	11.55	32.04	39.95	152.28	152.28	152..28
att. const. (dB/km)	0.29	0.009	0.01	0.02	0.02	0.02

3. Sheath Overvoltages in A Normal-Bonded Cable

3.1 Effect of fault conditions

(1) Core and sheath to ground fault

Fig. 3 shows a sheath overvoltage distribution along a normal-bonded cable due to a core and sheath to ground fault on phase "a" at the receiving end . ①(real line ——— in Fig. 3) is the case of the fault at the cable ① receiving end (node "AOUT1"), ② (— — —) at the cable ② end (node"DOUT1"), and ③ (—•—) at the cable ③ end (node "GOUT"). The highest overvoltage in each case is observed to be *89kV* at the node being next to the faulty node, i.e. node "AOUT2" in the case ①, and node " DOUT2" in the case ②on the faulty phase a, except the case ③. In the case ③, the highest overvoltage of *60kV* appears at node "FOUT" behind the faulty node "GOUT" because the next node to GOUT is grounded. The time of the highest overvoltage appearance is $t=\Delta t$ (computation time step). This indicates that the overvoltage appears right after the fault initiation at the nearest node due to the first traveling wave originated at the faulty node. When a ground fault occurs on the center phase "b", the overvoltage distribution characteristic is the same as the above.

When a ground fault occurs inside a cable at the position of 2x/3 from the sending end, the highest overvoltage is observed to be *60kV* at $t=2.4\ \mu s$ in the case of the cable ① fault and at $t=6.4\ \mu s$ in the cases of the cable ② and ③ faults, and appears at the nearest node behind the faulty position. The time of the maximum overvoltage appearance corresponds to the propagation time of a traveling wave from the faulty position to the node where the highest overvoltage appears.

Summarizing the above, the highest overvoltage of *89kV* appears on a cable sheath due to a core and sheath to ground fault. The overvoltage is higher in the case of a fault at the cable receiving end than in the case of a fault inside a cable. The highest overvoltage exceeds the insulation level of a *275kV* cable sheath.

(2) Core-to-sheath short-circuit fault

Fig. 4 shows a sheath overvoltage distribution due to a core-to-sheath metallic short-circuit fault of phase "a" at the receiving end. ①(real line ——— in the figure) is the case of the fault at the cable① node AOUT1, ②(— — —) at the cable② node DOUT1, and ③ (—• —) at the cable ③ node GOUT. The case③ shows no significant difference from that of the ground fault in Fig. 3 because the next node to the faulty node is grounded. In the cases ① and ②, however, the highest overvoltage reaches nearly *150kV* being far greater than that of the ground fault, and appears either at the faulty node or at the nearest node behind the faulty node. The reason for this is estimated that the core and the sheath at the faulty phase compose a metallic closed circuit with the source, in which a heavy fault current flows, and thus generates a very high overvoltage.

The above observation indicates that the metallic short-circuit fault may cause a severer damage to the sheath insulation and CCPUs of a cable than that due to a ground fault.

3.2 Effect of sheath grounding impedance

Fig. 5(a) shows the effect of a grounding resistance "R_g" on the sheath overvoltage distribution due to a core and sheath to ground fault with a constant grounding wire inductance of *3 μ H*. It is observed that all the sheath overvoltages increase as the grounding resistance increases. The highest overvoltage is 89kV when $R_g=0\ \Omega$, i.e. solidly grounded, and increases to *93kV/10 Ω* and *100kV/20 Ω*, which appears next to the faulty node. This is due to the fact that the overvoltage is proportional to the grounding

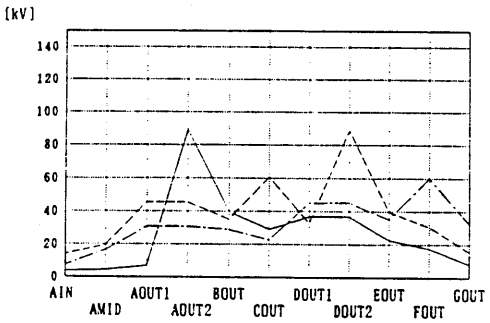

Fig. 3 Overvoltage distribution due to phase "a" to ground fault at the remote end on a normal-bonded cable.

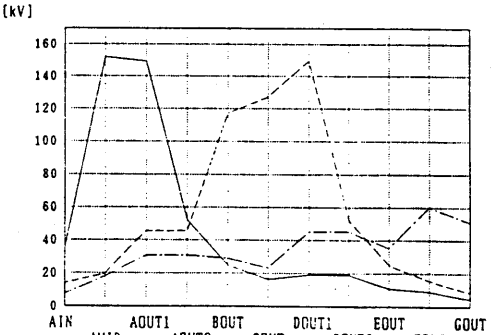

Fig. 4 Overvoltage distribution due to phase "a" core-to-sheath short-circuit fault.

resistance through which the fault current flows.

The effect of a grounding wire inductance L_g is shown in Fig. 5(b). The highest overvoltage increases from *58kV/L_g=1 μH* to *89kV/3 μH*, *110kV/5 μH* and *120kV/100 μH* as the inductance L_g increases.

When the cable sheaths are not grounded but isolated from the sheath, the overvoltage becomes far greater than that in the grounded case as expected from a circuit theory. The highest voltage appears on a sound phase "c" rather than the faulty phase "a". This can be explained as a result of a neutral voltage variation due to the fault current /2/.

In brief, the sheaths should be grounded to reduce the sheath overvoltage due to a fault, and the grounding resistance and the grounding wire length have to be made as small as possible.

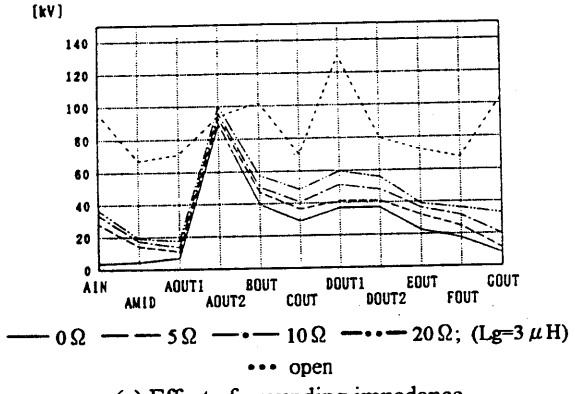

(a) Effect of grounding impedance

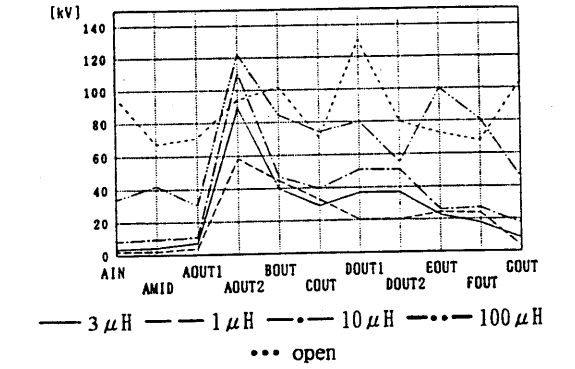

(b) Effect of grounding wire inductance

Fig. 5 Effect of grounding impedance

3.3 Analytical study of ground fault

The highest overvoltage has been observed to appear at the node next to the faulty node. The reason will be analytically studied in this section applying a distributed-parameter line theory /9/.

Fig. 6 shows transient current and voltage waveforms at the node "AOUT2" next to the faulty position in the case of the cable ① ground fault. It is clear that the current polarity changes every *75 μs* which is given as twice the propagation time of a traveling wave from the faulty node AOUT1 of the cable① to the remote end GOUT of the cable ③, i.e.

$$2\tau = 2(x_2 + x_3)/c = 2 \times 5700/152.8 = 74.6\mu s$$

The voltage waveform also shows a spike every *75 μs*.

The voltages v_g across the inductance L_g of the grounding wire is given in the following equation.

$$v_g = L_g \cdot di/dt \qquad (2)$$

For the derivative of the fault current i at the instance of the fault initiation is very large, the voltage v_g becomes very high. Fig. 7 illustrates an equivalent circuit of the faulty node/2/. Zc and Zs are the core to sheath and the sheath to earth surge impedances. Voltage source E corresponds the steady-state voltage just before the fault which is *224.5kV*. The sound phases are neglected in the analysis. The fault current I_g flowing from node "24" to the earth is given by:

$$I_g(s) = Z_s E\left[1/sZ_cZ_s - 1/\left\{1+Z_cZ_s/sL_g(Z_c+Z_s)\right\}\right] \qquad (3)$$

where s: Laplace operator

Laplace inverse transform of the above equation gives the following solution.

$$i_g(t) = (E/Z_c)\left[1-\exp\left\{-Z_cZ_st/L_g(Z_c+Z_s)\right\}\right] \qquad (4)$$

Substituting the above equation into eq. (2), the time response v_g is given by :

$$v_g(t) = \left\{Z_sE/(Z_c+Z_s)\right\} \exp\left\{-Z_cZ_st/L_g(Z_c+Z_s)\right\} \qquad (5)$$

The parameters of the above equation are :

E=-224.5kV, Lg=3 μH, Zc≒Zs=12.6 Ω,

t=$\triangle t$=0.2 μs

Substituting the above parameters, the following voltage is obtained.

vg=-78.8kV at t=$\triangle t$=0.2 μs

The above analytical result agrees satisfactorily with the highest voltage *-89.1kV* in the case of the cable ① ground fault calculated by the EMTP-ATP, and explains the generation of the highest voltage at the node next to the faulty node.

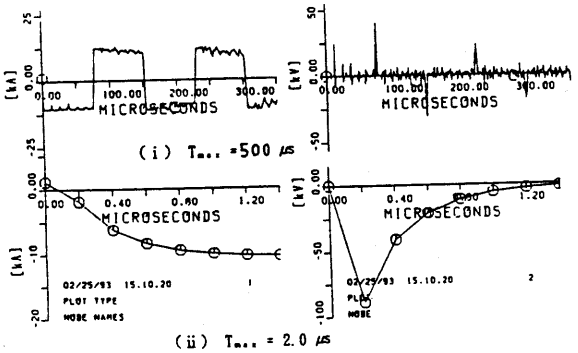

(a) Current (b) Voltage

Fig. 6 Phase "a" voltage and current waveforms at node AOUT2 for the cable ① ground fault

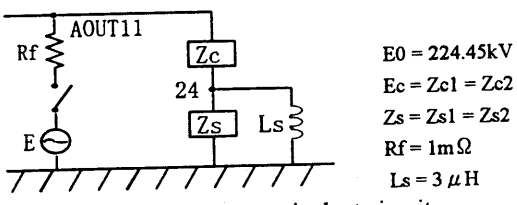

Fig. 7 An equivalent circuit

4. Sheath Overvoltages in A Crossbonded Cable

4.1 Ground fault

Fig. 8 shows the effect of cable crossbonding on sheath overvoltages due to a core and sheath to ground fault. In the figure, (a) ——— is the case of all the cable being normal-bonded, (b) — — — cable ② and ③ sheaths crossbonded, (c) • • • cable ② and ③ cores transposed, (d) —•— all the cables' sheath crossbonded, and (e) —••— all cables' cores transposed.

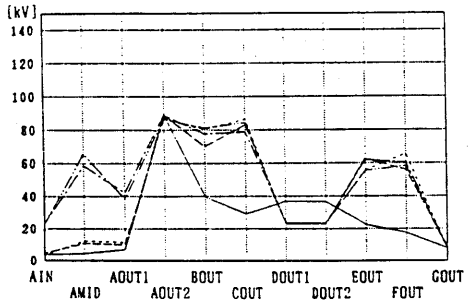

a) ——— ①,②,③ normal bonded
b) — — ②,③ sheath crossbonded
c) • • • ②,③ core transposed
d) —•— ①,②,③ sheath crossbonded
e) —••— ①,②,③ core transposed

Fig. 8 Effect of crossbonding

It is clear from the figure that most of the sheath overvoltages along the cable are grater in the crossbonded case than in the normal-bonded case as is well-known /9-11/. The highest overvoltage, however, is the same in the crossbonded and normal-bonded cables, and appears at the node next to the faulty node at the time right after the fault initiation. There is no significant difference between the cases of sheath crossbonding and core transposition.

The above is confirmed from transient current and voltage waveforms on the crossbonded cable (case b) shown in Fig. 9. It is observed in the figure that the transient waveforms until $t=12.5\ \mu s$ are the same as those in Fig. 6, although the waveforms for $12.5\ \mu s<t<500\ \mu s$ are quite different from those in Fig. 6 of a normal-bonded cable. For the highest overvoltage appears before $t=12.5\ \mu s$, no difference is observed between the normal-bonded cable and the crossbonded cable.

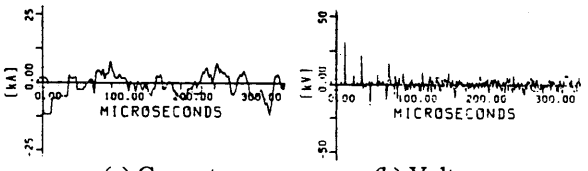

(a) Current (b) Voltage

Fig. 9 Phase "a" voltage and current waveforms at node AOUT2 in the crossbonded cable case

4.2 Effect of various parameters

(1) Fault position

Fig. 10 shows a comparison of sheath overvoltages due to a ground fault on the phase a at the receiving end. ① (——— in Fig. 10) is the case of the fault at the cable ① receiving end, ②(— — —)at the cable② receiving end, and ③(—•—) at the cable③ end. In the normal-bonded cable cases, the highest overvoltage tends to appear at the node next to the faulty node, while it shows no such the tendency in the crossbonded cable case. The reason for this is because a number of reflections and refractions of traveling waves at every crossbonded point produce high overvoltages at every node. This results in the highest overvoltage of 104kV in the cable ② fault case which appears on a sound phase (c). In general, the overvoltage is higher in the crossbonded cable than in the normal-bonded cable, and thus probability of sheath insulation breakdown is predicted to be higher in the crossbonded cable.

It is observed no significant effect of a faulty phase on a overvoltage distribution characteristic.

(2) Fault inside a cable

Fig. 11 shows sheath overvoltages when a fault occurs inside a cable at a position of 2x/3 from the sending end. A comparison of Fig. 11 with Fig. 10 makes clear that the overvoltages are higher by 50% in the case of a fault inside cables ② and ③ in the crossbonded cable, while the overvoltages are lower in the normal-bonded cable case.

(3) Metallic short-circuit fault

A core-to-sheath metallic short-circuit fault produces much higher overvoltages than those due to a ground fault as same as the normal-bonded cable case.

(4) Effect of grounding impedance

In the case of a ground fault at the cable① receiving end, the highest sheath overvoltage is $89kV/R_g=0\ \Omega$, i.e. the

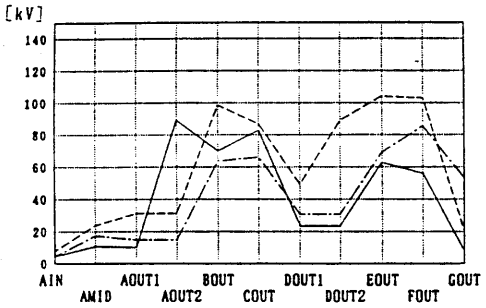

——— cable ①, — — cable ②
—•— cable ③ receiving end

Fig. 10 Overvoltage distribution due to a ground fault

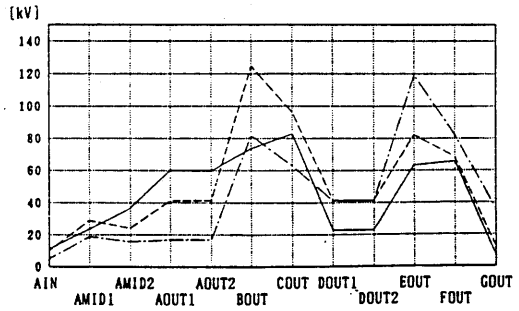

——— cable ①, — — cable ②
—•— cable ③ receiving end

Fig. 11 Overvoltage distribution due to a ground fault within a cable

solidly grounded case, *93kV/5 Ω*, *96kV/10 Ω*, and *100kV/20 Ω*, when the grounding resistance R_g is increased. The characteristic is the same as that in the normal-bonded cable case explained in Sec. 3.2. When the inductance of the grounding wire is changed, the overvoltage at the node next to the faulty node is *58kV/L_g=1 μH*, *89kV/3 μH*, *110kV/10 μH* and *122kV/20 μH*. The highest overvoltage appears at the second crossbonding node of the cable and is *81kV/1 μH* and *128kV/100 μH* which are greater than those in the above. This indicates that the highest overvoltage appears not necessarily at the node next to the faulty node, but the overvoltage at the node is the same as that in the normal-bonded cable. In other words, the overvoltage at the node is determined by the grounding wire inductance independently from a normal-bonded or crossbonded cable.

It is noteworthy that the overvoltage at the crossbonding points decrease as the grounding resistance increases.

5. Suppression of Sheath Overvoltages

5.1 CCPU

In the case of a ground fault at the cable① receiving end, sheath protection arresters (CCPU) are installed at the nodes where high overvoltages appear. Fig. 12 shows the effect of the number of the CCPUs. It is observed from the figure that the CCPUs suppress the sheath overvoltages less than the sheath insulation level except the highest overvoltage appeared next to the faulty node even though a CCPU(#1) is installed at the node. The reason for the highest overvoltage being not suppressed is that the overvoltage appears right after the fault initiation and the CCPU can not operate in such the short time period. Such the phenomenon is known as the fast impulse characteristic of an arrester /2,12/.

Fig. 13 shows absorbed energy by the CCPUs. The

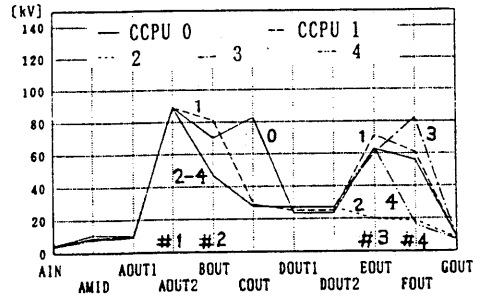

Fig. 12 Effect of the number of CCPUs

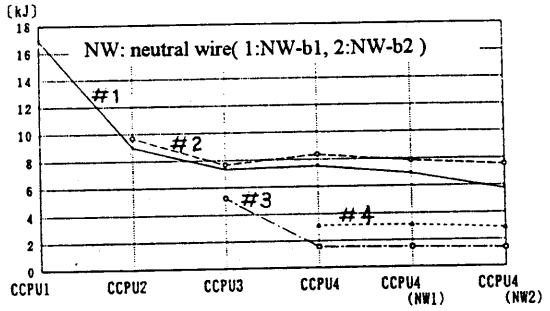

Fig, 13 Absorbed energy by CCPU

real line shows the absorbed energy by the first (#1) CCPU. When only one (#1) CCPU is installed at node AOUT2, the absorbed energy reaches about *17kJ*, and is reduced to *9kJ* by installing the second (#2) CCPU at node BOUT. The absorbed energy by the second CCPU is nearly *10kJ*, and is reduced to less than 8kJ by third (#3) CCPU installation at node EOUT. To reduce the absorbed energy less than *8kJ*, which is the limit of a modern ZnO arrester of a *60kV* class, 3 CCPUs at least have to be installed to avoid thermal breakdown of the CCPU. If a conventional SiC arrester is used, more than 4 CCPUs are to be installed, but the some of the CCPUs might be broken down thermally because the SiC arrester's capacity is less than *2kJ*.

5.2 Effecet of neutral wire

For the highest overvoltage appeared next to the faulty node may not be suppressed by a CCPU, an alternative approach to control the overvoltage is required from the viewpoint of sheath insulation . A neutral wire could be one possibility, and is investigated in this section.

Fig. 14 illustrates the cross-section and the configuration of a neutral wire, and Fig. 15 shows a schematic diagram of its arrangement. The neutral wire is grounded at each node where the cable sheath is grounded. When the neutral wire is installed only along the cable① in Fig. 1, no effect of the neutral wire on sheath overvoltages is observed. When the neutral wire is installed along the cables① and ②, a reduction of the sheath overvoltages by 9% in the cable① fault case and by 1% in the cable② fault case is observed as shown in Fig. 16(a). The effect of the neutral wire is more pronounced when the wire is installed nearby the faulty phase as is observed in Fig. 16(a) where the neutral wire is installed only along the cable②. It

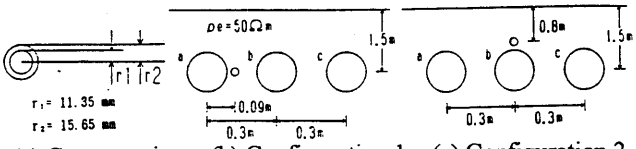

(a) Cross-section (b) Configuration 1 (c) Configuration 2

Fig. 14 Configuration of a neutral wire

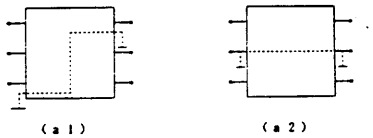

(a) Arrangement a : only cable ①

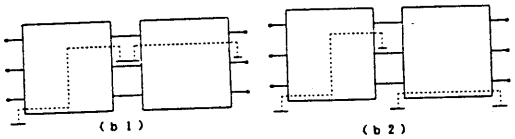

(b) Arrangement b : cable ①+cable ②

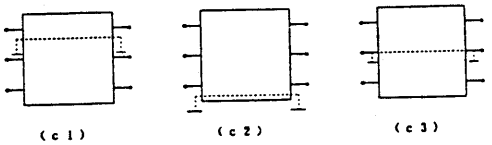

(c) Arrangement c : only cable ②

Fig. 15 Arrangement of a neutral wire

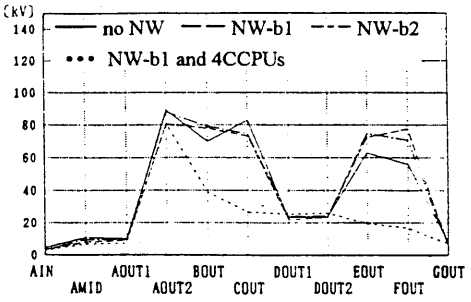

(a) Arrangement b in Fig. 15

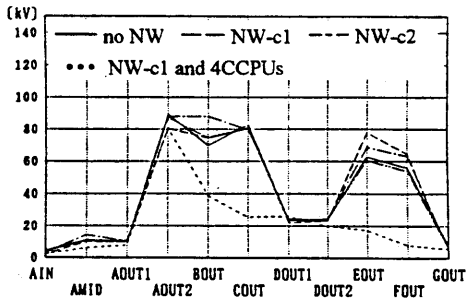

(b) Arrangement c in Fig. 15

Fig. 16 Effect of neutral wire

should be noted that the overvoltages in the cable③ sheath tend to increase when the wire is installed along the cables ① and/or ②.

A combination of the neutral wire and CCPUs is effective to suppress the sheath overvoltages as is observed in Fig. 16, but the suppression of the highest overvoltage is contributed only by the neutral wire. Also, energy absorbed by a CCPU is not reduced by the neutral wire.

6. Conclusions

Based on the investigation of sheath overvoltages on a *275kV* cable due to ground and metallic short-circuit faults, the following conclusions are obtained.

1) In the case of a core and sheath to ground fault at the receiving end of a cable, the highest overvoltage of *89kV* appears at the node next to the faulty position independently from a faulty phase and cable. The overvoltage exceeds the sheath insulation level *60kV* of the *275kV* cable and could cause breakdown of the sheath insulation and a sheath protection arrester CCPU. If a ground fault occurs inside a cable, the sheath overvoltage becomes smaller than the above in a normal-bonded cable, while it becomes grater in a crossbonded cable. Therefore, insulation breakdown is more probable in the case of a fault inside the crossbonded cable.

2) In the case of a core-to-sheath metallic short-circuit fault, the highest overvoltage reaches *150kV*, being much greater than that in the ground fault case, and appears at the faulty node or at the node behind it. Therefore, breakdown probability of sheath insulation is estimated to be much higher in the short-circuit fault case than in the ground fault case.

3) Sheath protection arresters CCPU suppress the sheath overvoltages less than the insulation level except the highest overvoltage, i.e. the CCPU has no effect to suppress the highest overvoltage. Energy absorbed by the CCPUs reaches more than 10kJ which exceeds the limit of both Sic and ZnO arresters with operating voltage of 60kV corresponding to the sheath insulation level of the *275kV* cable.

4) A neutral wire has a effect to reduce the highest overvoltage by about *9%* in the ground fault case and *1%* in the short-circuit fault case.

The investigations indicate that the sheath overvoltages due to a fault could even cause CCPU's breakdown and thus it is suggested to install a CCPU with greater energy capacity. Also, in a sheath insulation design, a care should be taken about the fact that the highest overvoltage appearing at the faulty node or the nearest node can not be suppressed by the CCPU and/or the neutral wire.

The observation is based of EMTP calculation results neglecting the frequency-dependent effect of a cable which affects transient overvoltages significantly. The effect of the frequency dependence on the highest overvoltage has to be investigated as a remaining problem.

References

1)J. P. Bickford, N. Mullineux and J. Reed : Computation of Power System Transients (IEE Monograph Series 18), Peter Peregrinus Ltd., 1976.

2)K. Ohhata, A. Ametani et.al. : Surge Phenomena and Countermeasures in Cable System, IEE Japan, Technical Report No.366, 1991.4.

3)L. M. Wedepohl and D. J. Wilcox : "Estimation of transient sheath overvoltages in pwer-cable transmission system", Proc. IEE, Vol.120(8), pp.877-822, 1973.

4)R. G. Wasley and S. Selvavinayagamoorthy : "Computation of sheath transient response in single-point bonded cable section", IEEE Trans., Vol. PAS-96, pp.248-254, 1977.

5)CIGRE SC21-WG07 : "Guide to the protection of specially bonded cable systems against sheath overvoltages", ELECTRA, No.128, pp47-61, 1990.1.

6)W. Scott-Myer : ATP Rule Book, Can/Am ATP Users' Group, 1993.

7)A. Ametani : CABLE PARAMETERS Rule Book, B.P.A., 1993.

8)N. Nagaoka and A. Ametani : "A development of a generalized frequency-domain transient program - FTP", IEEE Trans., Vol.PWRD3-(4), pp.1996-2004, 1988.

9)A. Ametani : Distributed-Parameter Line Theory, Corona Pub. Co., 1990.2.

10)L. M. Wedepohl and C. S. Indulkar : "Switching Overvoltages in short crossbonded cable systems using the Fourier transform", Proc. IEE, Vol.122(11), pp.1217-1221, 1975.

11)N. Nagaoka and A. Ametani : "Transient calculations on crossbonded cables", IEEE Trans., Vol. PAS-102(4), pp.779-784,1983.

12)J. Ozawa et.al. : Capability and Recent Testing Method of ZnO Arresters, IEE Japan Technical Report No.474, 1993.12.